Supporting information (SI)

$Mg_xCo_{1-x}(OH)_2$@C as electrode for supercapacitor: Effect of doping level on energy storage capability

Beina Yang [a, b], Bei Cheng [a], Huijuan Li [a], Tielin Wang [a] and Mingjiang Xie* [a,b]

a. Hubei Key Laboratory of Novel Reactor and Green Chemical Technology, Wuhan Institute of Technology, Wuhan 430205, China

b. Hubei Key Lab for Processing and Application of Catalytic Materials, Huanggang Normal University, Huanggang 438000, China

Supporting experimental details:

Samples characterizations: The crystallinity of the resultant products was analyzed by X-ray diffraction spectrometer (XRD) on LabX XRD-6100 (SHIMADZU) and Raman spectroscopy on Renishaw Invia Raman microscope. The surface chemistry including surface elemental composition and species was disclosed by X-ray photoelectron spectroscopy (XPS, Thermo Scientific ESCALAB). The morphology and microstructure of the resultant porous carbon were measured by scanning electron microscopy (SEM) on Zeiss Sigma 300 and transmission electron microscopy (TEM) on Thermo Fisher Talos F200X. Nitrogen adsorption/desorption isotherms conducted on Tristar 3020 were utilized to analyze the textual properties.

Supercapacitor test: Electrochemical measurements were carried out in a 6.0 M KOH aqueous electrolyte at room temperature, using a three-electrode cell with Hg/HgO as reference electrode and a platinum coil counter electrode. The working electrode was prepared by mixing the obtained samples powder, carbon black and polytetrafluoroethylene (PTFE) together at a mass ratio of 75:20:5, followed by coating the resulted mixture onto a nickel foam before being pressed together at 10.0 M Pa. The electrochemical performance of samples was determined by cyclic voltammetry (CV) and galvanostatic charge/discharge curves. The electrochemical properties of the asymmetric supercapacitor were investigated with a two-electrode cell

* Corresponding author. witwangtl@hotmail.com (T. Wang), xiemingjiang@smail.nju.edu.cn (M. Xie)

configuration with the obtained composite hydroxides as the positive electrode material, activated carbon (80% TF-B520, mixed with 10% carbon black and 10% PTFE) as the negative electrode material and polypropylene film as separator in 6.0 M KOH electrolyte solution. The mass ratio between the positive and negative electrodes was estimated according to the charge balance: $q_+ = q_-$. Cyclic voltammetry and galvanostatic charge-discharge were conducted on a CHI 660D electrochemical workstation (Shanghai CH Instrument Company, China). The specific capacitance of the asymmetric supercapacitor was calculated from the discharge curve according to the formula of

$$C_s = \frac{I\Delta t}{m} \text{ (C/g)} \qquad (1)$$

, where I is the current density (A), Δt is the discharge time (s), m is the total mass of the positive and negative electrodes,. The energy densities and power densities were calculated according to the formula of

$$E = \frac{1}{2} \times \frac{1}{3.6} CV \text{ (Wh/kg),} \qquad (2)$$

$$P = \frac{E}{t} \text{ (kW/kg)} \qquad (3)$$

where C (C/g) is the capacity of the asymmetric supercapacitor, V (V) is the working voltage of the cell, t is the discharge time.

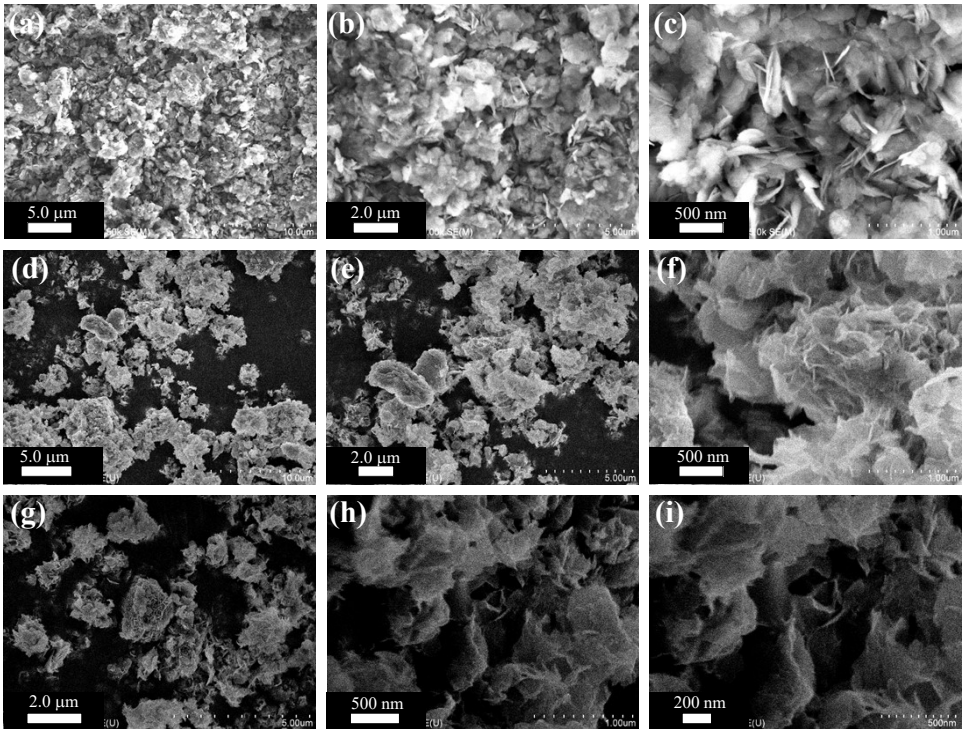

Figure S1. SEM micrographs of the resultant $Mg_xCo_y(OH)_2$ viewed at different magnifications. (a-c) $Mg_{0.8}Co_{0.2}(OH)_2$, (d-f) $Mg_{0.2}Co_{0.8}(OH)_2$ and (g-i) $Co(OH)_2$.

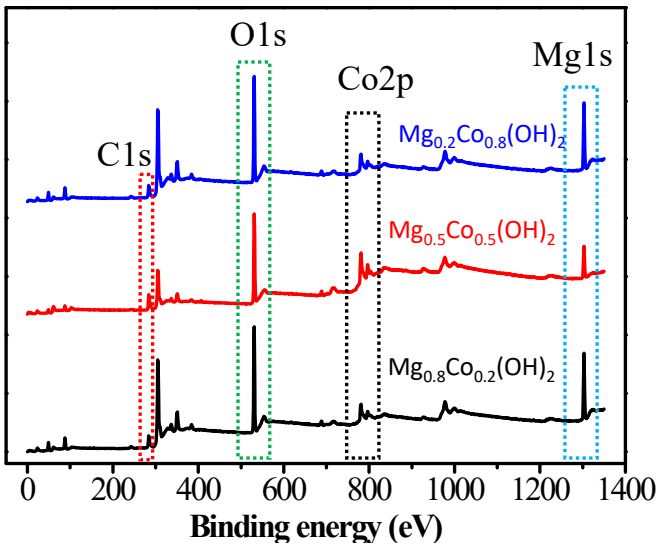

Figure S2. The survey XPS spectra of the resultant $Mg_xCo_{1-x}(OH)_2$.

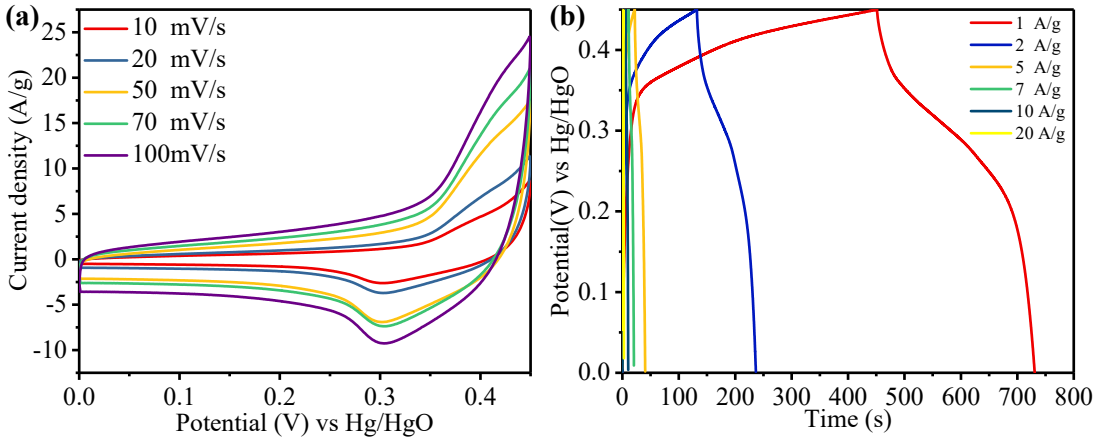

Figure S3. Supercapacitor performances of $Mg_{0.8}Co_{0.2}(OH)_2$ based electrode tested in three-electrode configuration. (a) CV plots and (b) GCD curves.

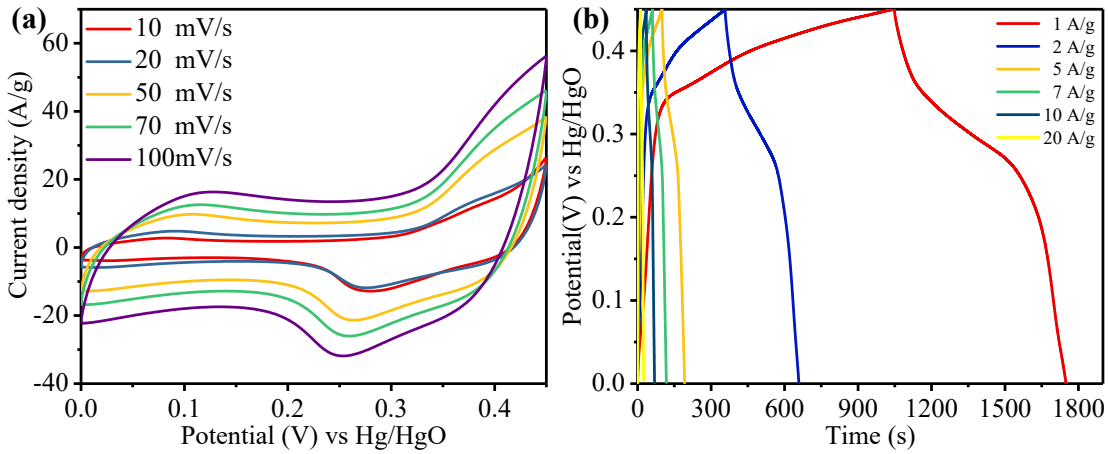

Figure S4. Supercapacitor performances of $Mg_{0.2}Co_{0.8}(OH)_2$ based electrode tested in three-electrode configuration. (a) CV plots and (b) GCD curves.

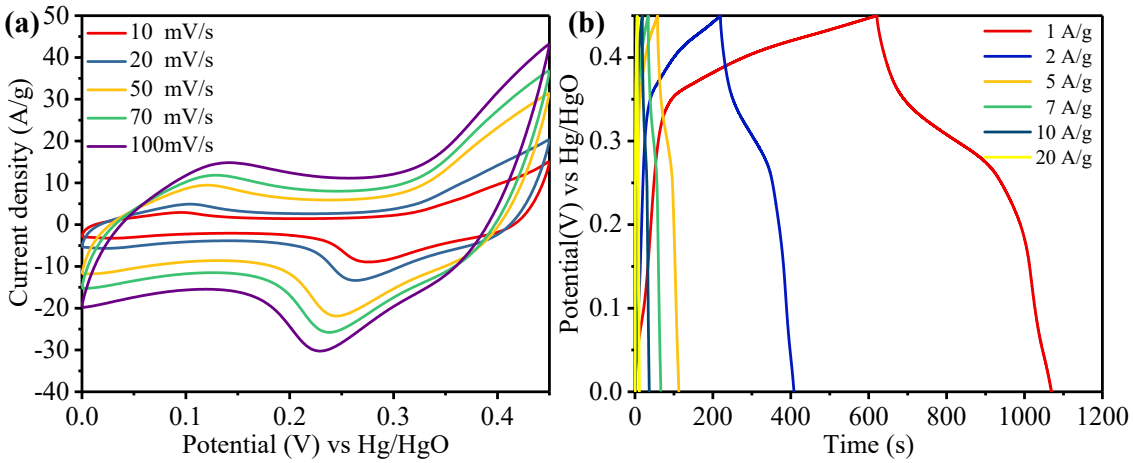

Figure S5. Supercapacitor performances of $Co(OH)_2$ based electrode tested in three-electrode configuration. (a) CV plots and (b) GCD curves.

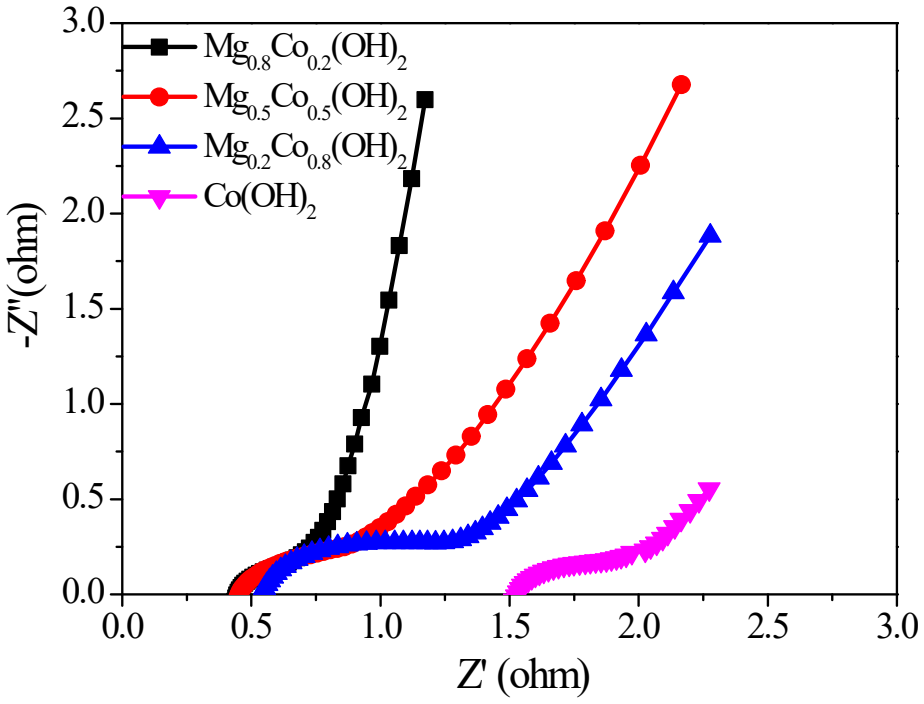

Figure S6. Nyquist plots of the resultant electrodes in three-electrode configuration.

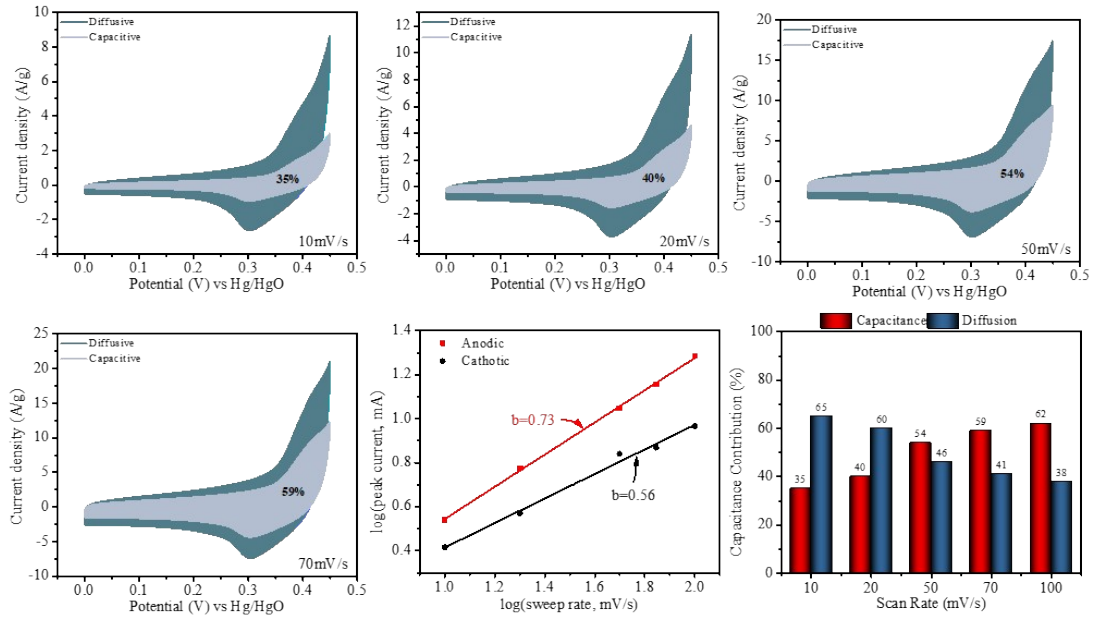

Figure S7. Capacitance contribution analysis of $Mg_{0.8}Co_{0.2}(OH)_2$ based electrode tested in three-electrode configuration.

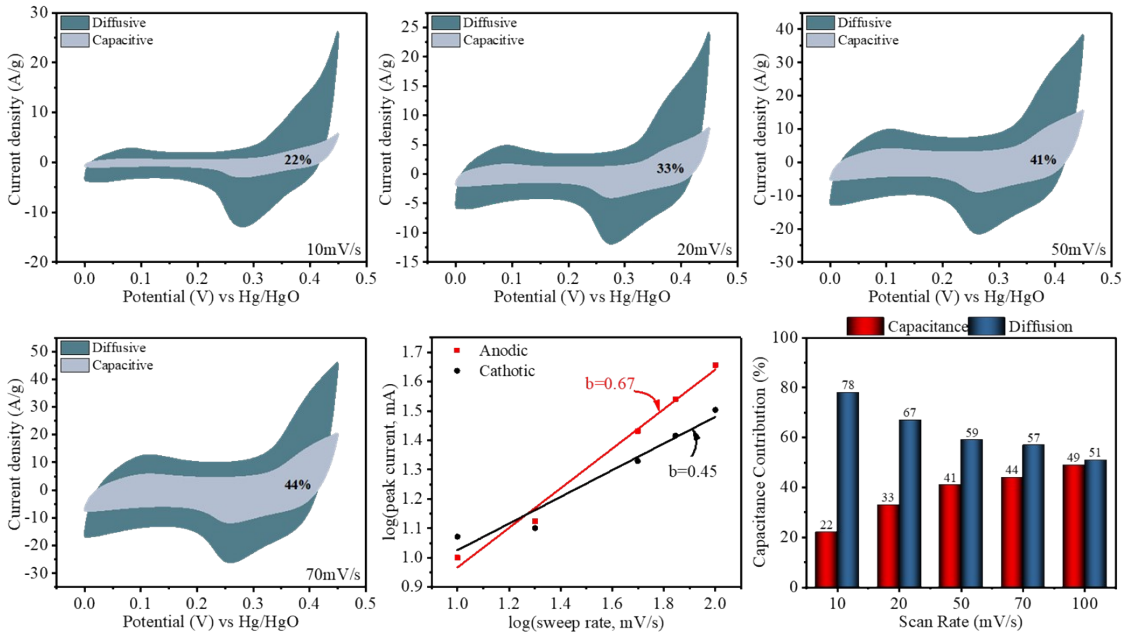

Figure S8. Capacitance contribution analysis of $Mg_{0.2}Co_{0.8}(OH)_2$ based electrode tested in three-electrode configuration.

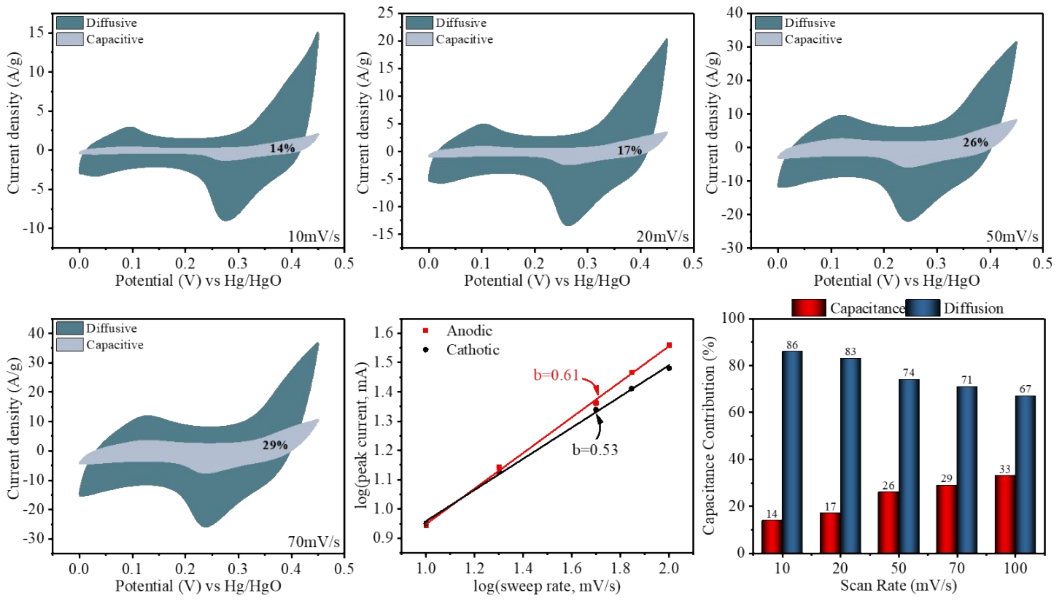

Figure S9. Capacitance contribution analysis of $Co(OH)_2$ based electrode tested in three-electrode configuration.

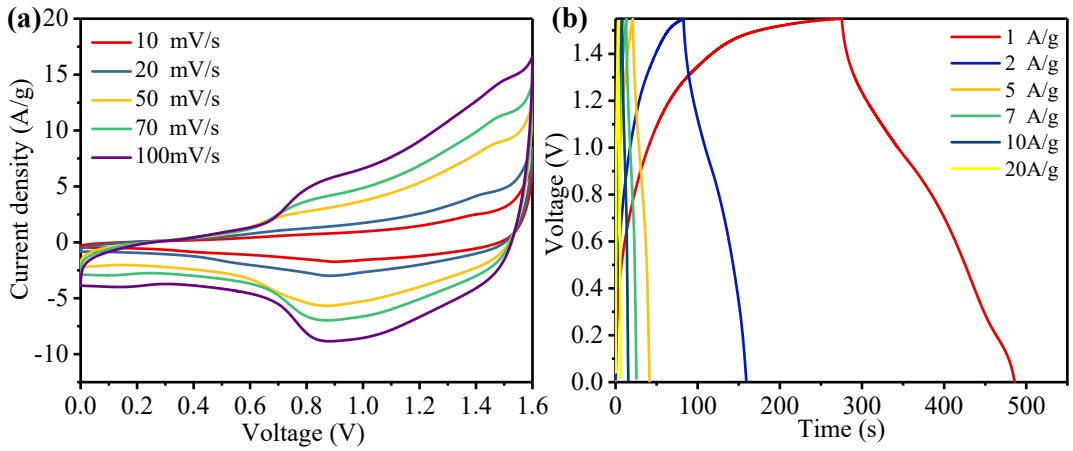

Figure S10. Supercapacitor performances of $Mg_{0.8}Co_{0.2}(OH)_2$ based electrode tested in asymmetric supercapacitor configuration. (a) CV plots and (b) GCD curves.

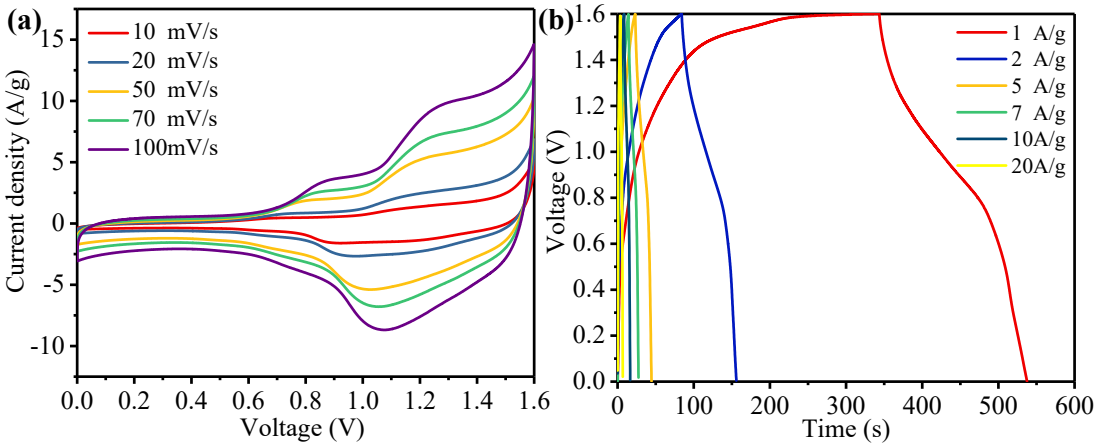

Figure S11. Supercapacitor performances of $Mg_{0.2}Co_{0.8}(OH)_2$ based electrode tested in asymmetric supercapacitor configuration. (a) CV plots and (b) GCD curves.

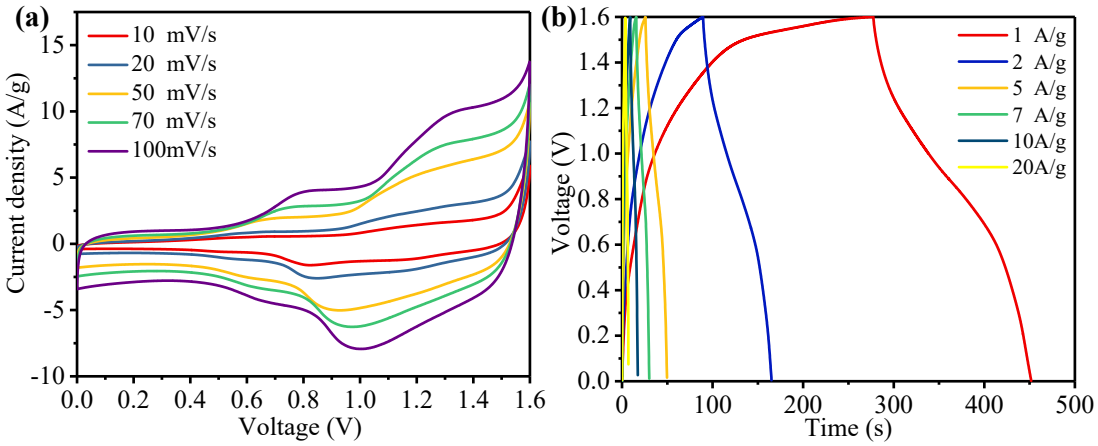

Figure S12. Supercapacitor performances of Co $(OH)_2$ based electrode tested in asymmetric supercapacitor configuration. (a) CV plots and (b) GCD curves.

Table S1. The asymmetric supercapacitor performance of the present work as compared to recently reported ones.

Electrodes	**Capacitance (F/g)**	**Electrolyte**	**Energy density (Wh/kg)**	**References**
$Mg_{0.5}Co_{0.5}(OH)_2$	**1193@1.0 A/g**	**6.0 M KOH**	**48**	**This work**
Ni-Co LDH-3	2369@0.5 A/g	2.0 M KOH	21.28	1
NiCo-LDH@rGO/NF	2408.8@0.5 A/g	1.0 M KOH	32.2	2

$Ni_{0.5}Co_{0.5}$LDH/AC	947@1.0 A/g	6.0 M KOH	39.7	3
$Co(OH)_2$/fCNT	432.7@0.4 A/g	PVA-KOH	17	4
$Co(OH)_2$-$MoSe_2$	541.55@1.0 A/g	6.0 M KOH	30.12	5
NF/MXene/CoAl-LDH	646.7@0.5 A/g	2.0 M KOH	45.11	6
CoMn(OH)F	541@1.0 A/g	3.0 M KOH	39	7
$Co(OH)_2$/SnO_χ/C	806.36@1.0 A/g	3.0 M KOH	49.73	8
$Co(OH)_2$@PANI	385@1.0 A/g	6.0 M KOH	31.2	9
L-MCH	1312.88@10A/g	4.0 M KOH	55.75	10

Supporting references:

[1] M. Wang, Y. Feng, Y. Zhang, S. Li, M. Wu, L. Xue, J. Zhao, W. Zhang, M. Ge, Y. Lai, J. Mi, Ion regulation of hollow nickel cobalt layered double hydroxide nanocages derived from ZIF-67 for High-Performance supercapacitors, Applied Surface Science, 596(2022) 153582.

[2] Z. Yang, Q. Cheng, W. Li, Y. Li, C. Yang, K. Tao, L. Han, Construction of 2D ZIF-derived hierarchical and hollow NiCo-LDH "nanosheet-on-nanosheet" arrays on reduced graphene oxide/Ni foam for boosted electrochemical energy storage, Journal of Alloys and Compounds, 850(2021) 156864.

[3] T. Chen, L. Luo, X. Wu, Y. Zhou, W. Yan, M. Fan, W. Zhao, Three dimensional hierarchical porous nickel cobalt layered double hydroxides (LDHs) and nitrogen doped activated biocarbon composites for high-performance asymmetric supercapacitor, Journal of Alloys and Compounds, 859(2021) 158318.

[4] R. Ranjithkumar, S. E. Arasi, P. Devendran, N. Nallamuthu, A. Arivarasan, P. Lakshmanan, S. Sudhahar, M. K. Kumar, Investigations on structural, morphological and electrochemical properties of $Co(OH)_2$ nanosheets embedded carbon nanotubes for supercapacitor applications, Diamond and Related Materials, 110(2020) 108120.

[5] A. Alam, G. Saeed and S. Lim, One-step synthesis of 2D–2D $Co(OH)_2$–$MoSe_2$ hybrid nanosheets as an efficient electrode material for high-performance asymmetric supercapacitor, Journal of Electroanalytical Chemistry, 879(2020) 114775.

[6] S. Ma, W. Wang, X. Che, Q. Ren, Y. Li, C. Hou, Fabrication of nickel foam/MXene/CoAl-layered double hydroxide by electrodeposition as electrode material for high-performance

asymmetric supercapacitor, Synthetic Metals, 305(2024) 117613.

[7] T. T. Nguyen, J.-J. Shim, Formation of fringed carnation-like cobalt manganese fluoride hydroxide assisted by ammonium fluoride for supercapacitor applications, Journal of Power Sources, 521(2022) 230888.

[8] Y. Li, J. Ma, S. Yang, L. Cui, H. Lu, One-step synthesis of $Co(OH)_2/SnO_\chi$/C hybrid nanosheets for asymmetric solid-state supercapacitors, Journal of Alloys and Compounds, 881(2021) 160508.

[9] A. Keshavarz, J. Tashkhourian, S. F. Nami-Ana, Designing an asymmetric supercapacitor based on $Co(OH)_2$@PANI nanocomposite synthesized via a facile hydrothermal method, Journal of Energy Storage, 73(2023) 108825.

[10] A. Nanwani, K. A. Deshmukh, P. Sivaraman, D. R. Peshwe, I. Sharma, S. J. Dhoble, H. C. Swart, A. D. Deshmukh, B. K. Gupta, Two-dimensional layered magnesium–cobalt hydroxide crochet structure for high rate and long stable supercapacitor application, npj 2D Materials and Applications., 3(2019), 45.